OBSERVATIONS OF ATMOSPHERIC SOLITARY WAVES IN THE URBAN BOUNDARY LAYER

M. P. RAO[2], PAOLO CASTRACANE[1], STEFANO CASADIO[1], DANIELE FUÀ[3] and GIORGIO FIOCCO[1]

[1]*Department of Physics, Università di Roma La Sapienza, 00185 Roma, Italy;* [2]*Department of Physics, Andhra University, 530003 Visakhapatnam, India;* [3]*DISAT, Università di Milano-Bicocca, 20126 Milano, Italy*

(Received in final form 6 March 2003)

Abstract. The simultaneous operation of a three-axis Doppler sodar system in the central urban area of Rome and two similar systems in the suburban area, forming a triangle about 20 km on each side, provided evidence of solitary-type waves in the urban boundary layer. Three events, each lasting from a few minutes to about 30 min, and ranging in depth from the minimum range of the sodar (39 m) to over 500 m, are reported here. Two events were recognizable on all three sodar records while the third event could be observed at the urban location only. Time-height acoustic echo intensity records showed no-echo regions within the wave indicating transport of trapped recirculating air. This is typical of large amplitude solitary waves. The time series plots of sodar-derived vertical wind velocity revealed a maximum peak-to-peak variation of about 5 m s^{-1} during periods of wave-associated disturbance. The vertical velocity is found to increase with height up to the top of the closed circulation within the wave and decreases further above. The normalised amplitude-wavelength relationship for the two events indicates that the observed waves are close to a strongly nonlinear regime.

Keywords: Gravity waves, Nonlinear waves, Sodar, Solitary waves, Solitons, Urban boundary layer.

1. Introduction

Many observational studies of solitary waves in the atmospheric boundary layer (ABL) have been based on datasets obtained in Australia and America. The well-known 'morning glory' phenomenon in northern Australia in spring, in the form of roll clouds often having lengths of few hundred kilometres, is a visual manifestation of solitary waves when the lower atmosphere is both stable and moist. These waves usually travel at an estimated speed of over 10 m s^{-1} with amplitudes of several hundred metres and wavelengths of a few kilometres (Christie, 1992; Rottman and Einaudi, 1993; Menhofer et al., 1997). A thunderstorm-generated solitary wave of 400 m amplitude and 2000 m wavelength propagating at 13 m s^{-1} in an inversion layer of 500 m depth was observed in the central Oklahoma region (Doviak and Ge, 1984; Doviak et al., 1991). The wave travelled about 100 km from its source. Fulton et al. (1990) observed another event in the same Oklahoma area that was believed to be associated with the early stage in the development of a solitary wave family.

Boundary-Layer Meteorology **111:** 85–108, 2004.

Satellites and other space-based cameras aided in the detection of solitary waves at other geographical locations such as the gulf coast of Texas and the Arabian Sea (Clarke, 1998; Zheng et al., 1998; Szantai et al., 2000). A few observational studies on solitary waves of relatively modest amplitudes are available from the Antarctic ABL. Rees and Rottman (1994) analysed several solitary waves with phase speeds ranging between 2 and 10 m s^{-1} propagating from land over a gently sloping coastal Antarctic ice shelf. These waves, with wavelengths of the order of 200 m and amplitudes below 40 m, are known to occur only when the prevailing wind speeds are low.

In general, the amplitude of a solitary wave is inferred from pressure or temperature fluctuations measured at ground level or at some higher levels in the atmosphere. It is known that estimation of wave amplitude from such point sensor measurements is difficult (Rottman and Einaudi, 1993; Rottman and Grimshaw, 2001). On the other hand, measurements with ground-based remote sensing systems, such as wind profilers, RASS, lidar or Doppler sodar, are expected to provide snapshots of the evolving phenomena in both time and height (Doviak and Ge, 1984; Rottman and Einaudi, 1993; Clifford et al., 1994). A monostatic Doppler sodar should be useful in making measurements related to solitary waves as the facsimile record, in the form of a time-height plot of echo intensity, provides the amplitude information directly when the waves are propagating below about 1 km height and most conventional sodars work well up to that height. The sodar signature of solitary waves is obtained from sound scatter at the interface between the ambient air and the recirculating air within the wave. The maximum height of the echo region on the sodar facsimile record during the event provides a measure of the wave amplitude (Cheung and Little, 1990). Solitary wave studies using sodar as one of the measuring instruments are few. Christie et al. (1981) presented two solitary wave events detected by a monostatic sodar operated at Warramunga (Australia). The number of solitary waves in each event and their amplitudes were directly measured from the sodar facsimile records. As many as seven solitary waves were identified in one event. The amplitudes ranged between 200 and 400 m with wavelengths of over 1000 m. By operating a high-resolution sodar with a maximum range of 100 m along with a conventional sodar, Cheung and Little (1990) observed five solitary wave events with amplitudes up to 500 m that were propagating in a shallow stable nocturnal boundary layer at Boulder in the U.S.A. Solitary waves propagating in the marine boundary layer off the coast of southern California (U.S.A.), with amplitudes as low as 25 m, were observed by a low-minimum range monostatic sodar aboard ‘Point Sur’ (Cheung et al., 1990).

The urban boundary layer (UBL) is known for its unstable characteristics all through the day except for the few hours before dawn (Ching, 1985; Oke, 1987; Casadio et al., 1996). The requirement of a stable boundary layer for the generation or propagation of solitary waves may not always be fulfilled in the UBL. However, under certain meso-meteorological circulations, as in the three events reported here, a moderately stable UBL may exist and support the propagation of solitary

waves. While two events are believed to be associated with thunderstorm outflow or drainage flow, the third event occurred during a synoptic-scale disturbance. The mechanisms involved in waveguide establishment in the UBL during the events are different. Although the present data set is limited to Doppler sodar measurements at three locations and a reconstruction of the full horizontal section through the disturbance is not possible, the roughness of the urban canopy appears to have a bearing on the propagation characteristics of the observed solitary waves. The results are in agreement with some of the fully nonlinear theory predictions and previous studies made at other locations, but the significance of the observations presented here lies in the rarity of the occurrence of the phenomenon in the UBL.

2. Experiment and Site Location

The experiment was part of an observational program related to the urban heat island and low level wind field regimes in the Rome region. The three Doppler sodar systems used in the present experiment have similar characteristics and were operated in the monostatic mode with a maximum operational range of 800 m. Each system consisted of three 1.2 m parabolic antennae; two of them were tilted 20° from the vertical, one pointed to north and the other to east, while the third was pointed to zenith. The three antennae radiated simultaneously 100 ms long acoustic tones centred at 1750, 2000 and 2250 Hz respectively, allowing a vertical resolution of 27 m in the measurements. The signals received on the three antennae were mixed before analysis, using a digital signal processor card plugged into the PC bus. The Doppler shift and the echo intensity were retrieved by employing a two-step procedure to increase the accuracy of measurements (Mastrantonio and Fiocco, 1982). A more detailed description of the system and other data analysis techniques are available elsewhere (Mastrantonio and Argentini, 1997).

A map showing the main geographical features of the region around the three experimental sites is presented in Figure 1. The locations of the three Doppler sodar systems are marked as U (University), M (ponte Malnome) and P (Pratica di mare). The shaded regions in the map are the metro area of Rome and the densely populated areas in the suburbs. The city is in the lower Tiber valley with mountains on all sides except towards the sea. The sodar system at U is in a highly urbanised commercial downtown area of Rome. All three sodar systems are approximately at the same height of around 60 m above sea level. The positioning of the three sodar systems forms a triangle with sides of length 17 km, 23 km and 26 km for UM, MP and UP respectively.

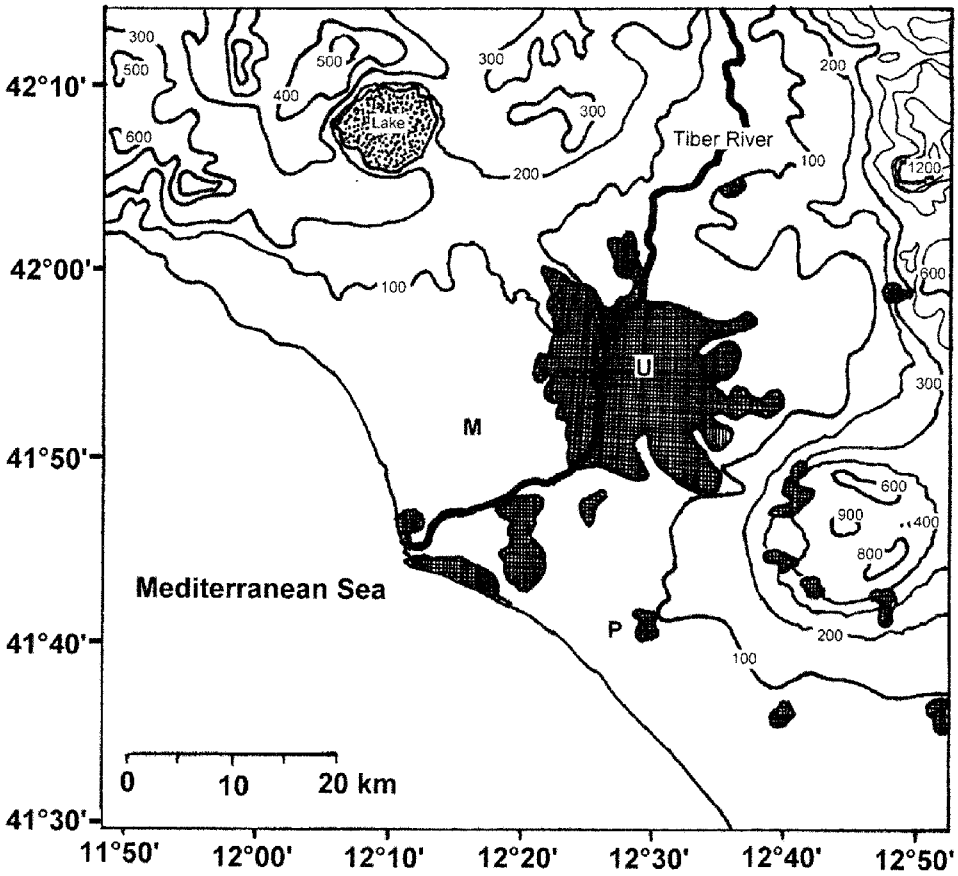

Figure 1. The map of Rome and its surroundings. The shaded parts are the metro area and the densely populated areas in the suburbs. The locations of the three Doppler sodars are marked by U (University), M (ponte Malnome) and P (Pratica di mare).

3. Results and Discussion

The selection of the cases is based on visual examination of facsimile records obtained at the three locations. When one of the records shows large amplitude waves with a very weak or no echo region within the waves, the facsimile records at the other two locations are scrutinized. A case is said to be identified when the wave packet appears at the other two locations within about a 2-hr period. Three such events, two in spring and one in autumn, observed by the Doppler sodar network are presented in the following sections.

The discussion of the results relies heavily on interpretation of the facsimile records along with the vertical and horizontal wind profiles obtained with the three Doppler sodars. Unfortunately, no simultaneous surface meteorological measurements are available at any of the three locations. Routine temperature and relative

humidity measurements made by the UCEA (Central Office of Agricultural Ecology) station, about 2 km west of location U, are available, but the precision and the time resolution are inadequate for this study. Nevertheless, they confirmed the events related to thunderstorm cold outflows and are mentioned in the following sections, whenever recognizable variations were observed.

3.1. CASE 1: APRIL 15–16, 1996

The surface weather charts of April 15 at 1300 local time showed instability conditions over eastern parts of Italy and an increasing trend in surface pressure over the central Mediterranean sea. The weather forecast for the day included thunderstorms in the hinterland and some scattered rainfall in southern parts and the lower Adriatic sea. The sodar facsimile records (not shown here) at the three locations showed vigorous convective activity during the daytime (April 15). The surface relative humidity and temperature (not shown here) also showed large variation. The relative humidity changed from the previous night maximum of 80% to a daytime minimum of 14% while the temperature underwent a change of about 10 °C.

Meteosat images for the evening period showed thunderstorm activity in some parts of central Italy, but there were no thunderstorm or rain reports in Rome. However, thunderstorms were reported at Grosseto (150 km north-west of Rome) and Monte Terminillo (75 km north-east of Rome). The two-hour sections of the three sodar facsimile records presented in Figure 2 show the effects of a cold outflow over the experimental area. In general, sodar records during fair weather conditions around this time of the day (sunset at 1851) are featureless, as the boundary layer is in its transition from daytime convective activity to the nocturnal stable regime. The outflow current appeared first at location U around 1830 producing a stable layer up to about 300 m height (Figure 2a). The relative humidity showed a sudden decrease of 8% during this time. The cold outflow appeared at location M almost an hour later at around 1930 as revealed in Figure 2b. The stable layer extended up to about 400 m height. The record at location P (Figure 2c) is a classical depiction of typical thunderstorm cold outflows (Hall et al., 1976). The arrival of the outflow current was marked by a sudden rise of the layer up to about 500 m between 2020 and 2035. The Doppler sodar horizontal wind profiles (not shown here) during the cold outflow at the three locations showed winds with speeds up to 8 m s^{-1} from north-north-west or north. Thus, the experimental area was under the influence of cold outflow for about an hour which established a stable layer of few hundred metres depth in the UBL.

3.1.1. *Location U*

The three-hour section of sodar facsimile record from 2300 (April 15) to 0200 (April 16) is shown in Figure 3a and shows echoes up to 200 m height for about 30 min from 2300. Shortly after 2330, an elevated layer, which first appeared at

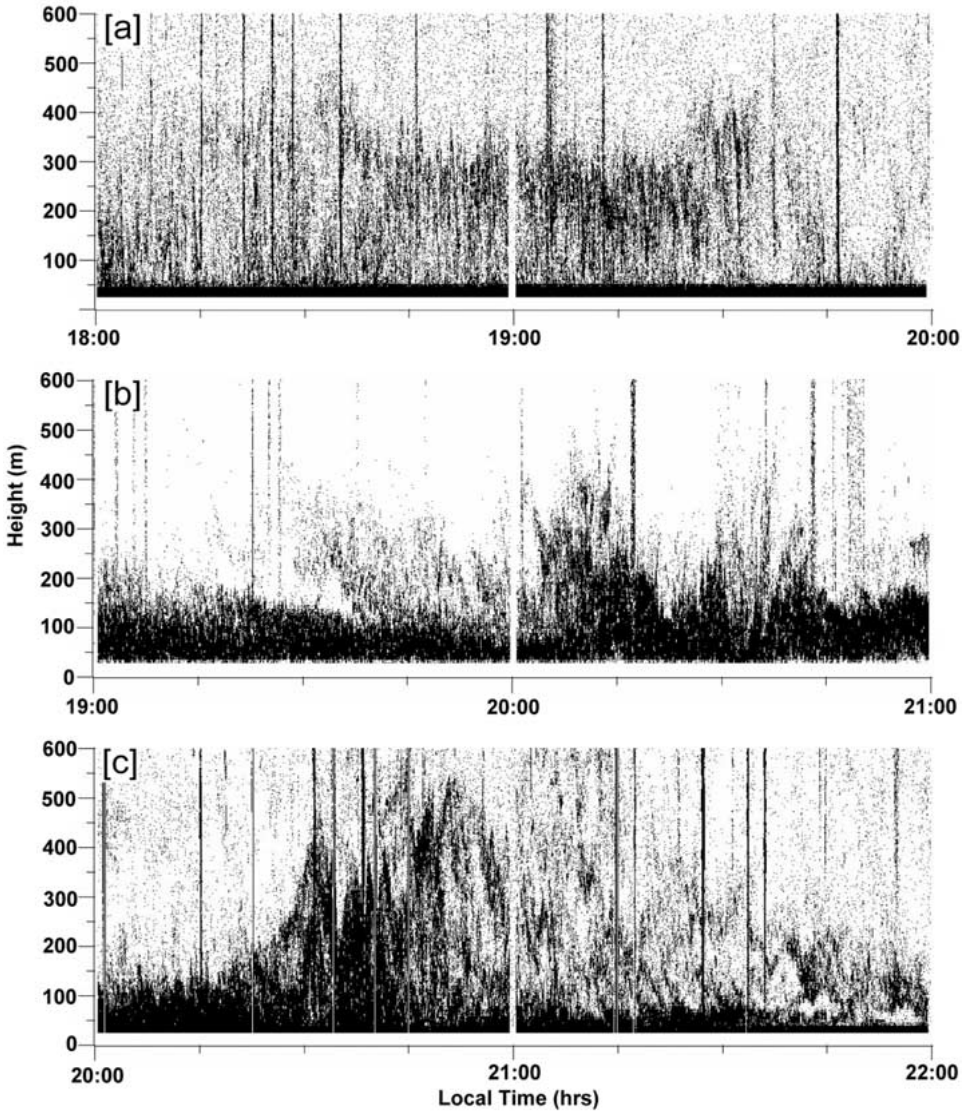

Figure 2. Sodar facsimile records showing thunderstorm outflow-related structures, a few hours before the occurrence of waves, at the three locations U, M and P, respectively (a), (b) and (c) on April 15, 1996

around 450 m, began descending at an average rate of about 0.1 m s^{-1}. The elevated layer underwent large undulations during its descent. The more interesting part of the facsimile record is from 0010 when waves of amplitudes ranging between 350 m to 550 m began to appear. At about 0010, the surface-based echo region started rising to above 250 m with a corresponding rise of the elevated layer to well above 400 m. The two echo regions were separated by a clear no-echo region

of about 20 m thickness. Both the layer and the lower scattering region descended as quickly as they rose, and several cycles of this rise and fall followed. The facsimile record from 0050 shows several small amplitude waves till the end of the record, but only those with a clear no-echo region are marked as S1 to S5 and form part of further analysis presented in later sections. The waves appear to be amplitude-ordered with S2 and S5 having amplitudes of 550 m and 400 m respectively. Cheung and Little (1990) interpreted these no-echo regions within the waves as an acoustic signature of solitary waves with recirculating cells that transport air from the initiating disturbance. The recirculating cells are known to continuously mix the air within the cells as the wave moves away from its origin, and thus become acoustically smooth by lacking necessary temperature gradients for sound scattering. The sodar facsimile records shown by Christie et al. (1981) also revealed these no-echo regions within a train of solitary waves, which were believed to be associated with the morning glory phenomenon.

The time series of vertical velocity at ten representative heights for the three-hour period is presented in Figure 3b. The vertical velocity was measured for each scan (6 s) and no time-averaging or smoothing was performed on the data presented in Figure 3b. The gaps in the time series represent missing data points (see for example, 230 m and above up to 2345 from the beginning) due to inadequate signal-to-noise ratio. The variations in vertical velocity were small at all heights until the arrival of solitary waves at 0010. The large fluctuations at and above 230 m height, for a period of an hour from the beginning of the series, were associated with undulations of the descending elevated layer. During each soliton from 0010, the vertical velocity initially rose to a positive peak followed by a smooth decrease through zero to a negative peak value. This pattern was observed in solitons marked S1 through S5 on the facsimile record (Figure 3a). The peak values of vertical velocity were decreasing from S3 onwards indicating that the waves were indeed amplitude-ordered as revealed by the facsimile record and mentioned earlier. The reason for some minor fluctuations in vertical velocity between S1, S2 and S3 is less clear. It may be noticed from Figure 3b that the peak positive velocities were higher compared to the peak negative velocities at almost all levels; the peak positive velocities were close to 3 m s^{-1} while the peak negative velocities seldom crossed 2 m s^{-1}. This is unusual for solitary waves, as theoretical models and most of the earlier observational studies reported almost equal peak positive and negative vertical velocities (Christie and Muirhead, 1983; Rottman and Einaudi, 1993; Cheung and Little, 1990). The analysis of a thunderstorm-triggered solitary wave event, observed by a 444 m meteorological tower and a Doppler radar in the Oklahoma area, by Fulton et al. (1990) suggest that the higher positive velocities are an indication of evolving solitary waves. It appears that the sodar facsimile record presented in Figure 3a displayed several features of the schematic diagram presented in Figure 6 of Fulton et al. (1990). It is known that density currents develop a nose shaped frontal region in response to surface friction. The observation of the sudden appearance of the elevated layer at around 2300 and its

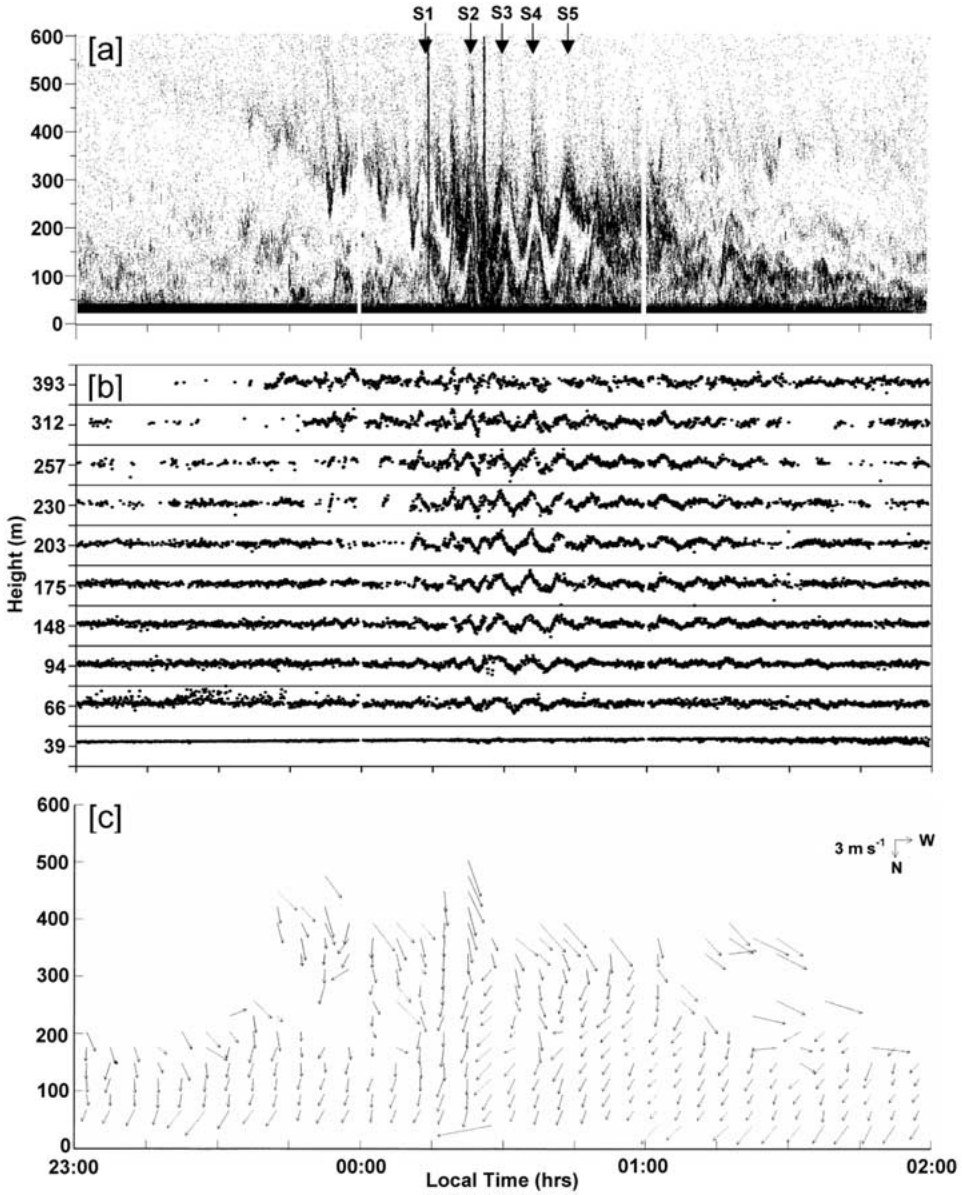

Figure 3. (a) sodar facsimile record, (b) time series of vertical wind for ten representative heights and (c) horizontal wind field for 3 h from 2300 (April 15, 1996) to 0200 (April 16, 1996) obtained at location U. The centre tick mark at each height in (b) is 0 m s^{-1}, while the upper and lower tick marks are $+3$ m s^{-1} and -3 m s^{-1}, respectively.

later descent to lower levels resemble the features of the nose in a density current, although the horizontal extent of the transition in the present observations seems to be long. This can be attributed to the high friction of the urban canopy, which can retard the flow more than a natural surface. It may thus be considered that the solitary waves in the present observations were in their developmental stage and were part of the gravity current.

The horizontal wind field presented in Figure 3c is based on 5-min averaged profile measurements. The winds were mostly from north with speeds up to 6 m s^{-1}. The winds during the wave event were variable in direction from north to north-east. The winds remained steady after the event and are from the north-east.

3.1.2. *Location M*

The sodar facsimile record presented in Figure 4a for the period 2300 (April 15) to 0200 (April 16) shows intense scattering up to 200 m for about 30 min from the beginning of the record. A weak but recognizable layer from heights above 500 m was seen descending during the same period. The scattering at lower levels rose to heights above 300 m for about ten minutes from 2330. The scattering then became diffuse and the height of scattering was variable till the end of the record. The more interesting part of the record is from 0030 to 0035 during which a single wave-like structure appeared with a clear no-echo region in the form of an elongated ellipse (marked as S1) between 100 and 250 m height. The time series of vertical velocity presented in Figure 4b shows that the variation was similar to those shown earlier at location U (Figure 3b), albeit on a smaller scale. The peak positive and negative velocities were about ± 1 m s^{-1}.

The horizontal wind field shown in Figure 4c shows that the winds were from west and northwest till 2330, when the elevated layer reached the lower scattering regions. The winds were light and variable afterwards. During the wave event and the remaining period of the record, winds below 300 m were from north with occasional turning to north-east. The winds at higher levels continued from the north-west.

3.1.3. *Location P*

The sodar facsimile record for the period 0100 to 0400 (April 16) presented in Figure 5a shows three weak elevated layers between 100 and 500 m height till about 0205. The top layer, with large undulations, was seen descending and appeared similar to that observed at location U (Figure 3a) before the arrival of solitary waves. The intense scattering from 0210 for a period of 15 min extending up to 550 m height (marked as S1 and S2) appeared to be amplitude-ordered, but devoid of any wave-type appearance. The facsimile record for the rest of the period showed multiple layers. The time series of vertical velocity for the corresponding period (see 257 and 284 m levels) shows that there were at least two waves in the disturbance (Figure 5b). The magnitude of vertical velocity variation during the wave-associated disturbance was less than at location U (Figure 3b).

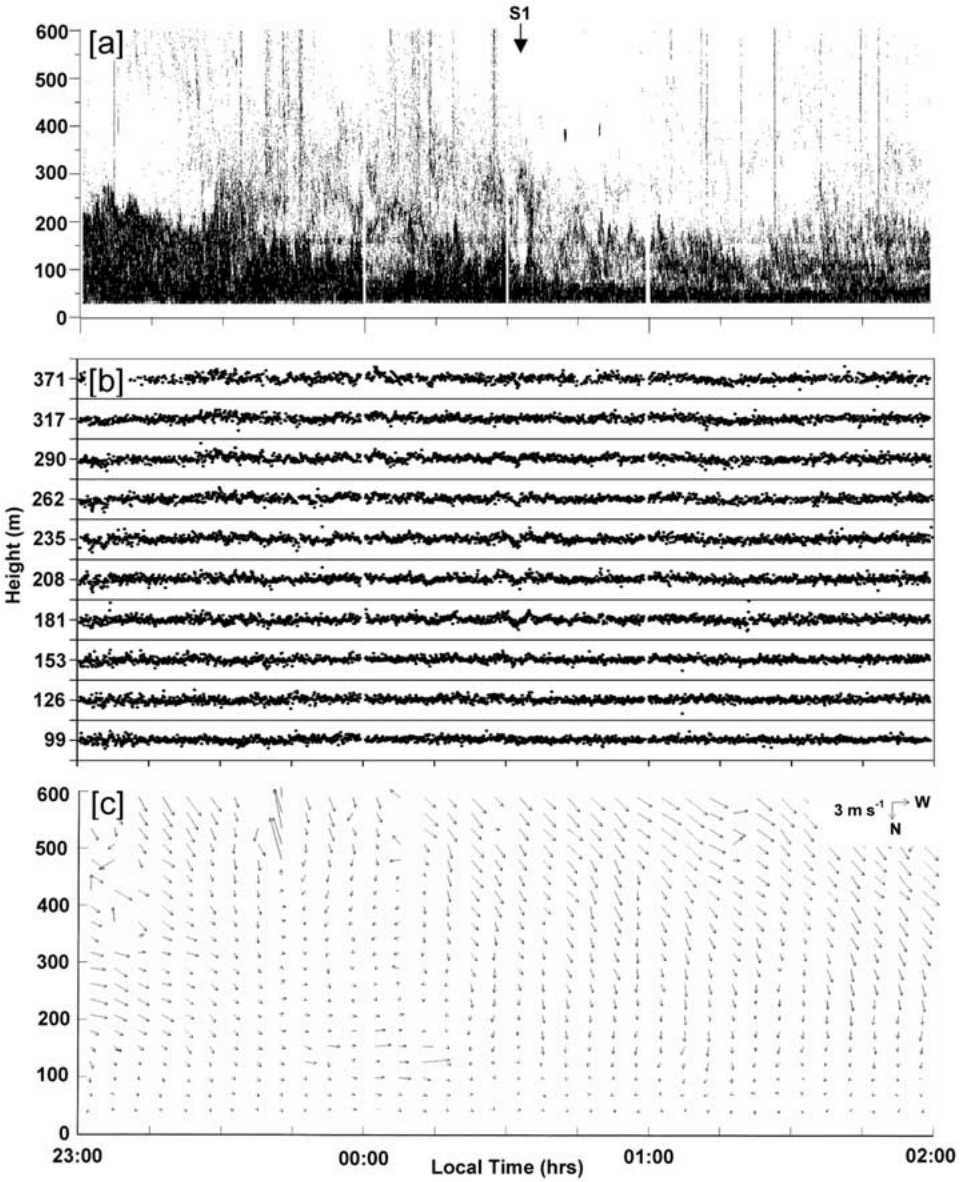

Figure 4. Same as Figure 3 but for location M. The centre tick mark at each height in (b) is 0 m s^{-1}, while the upper and lower tick marks are +2 m s^{-1} and −2 m s^{-1}, respectively.

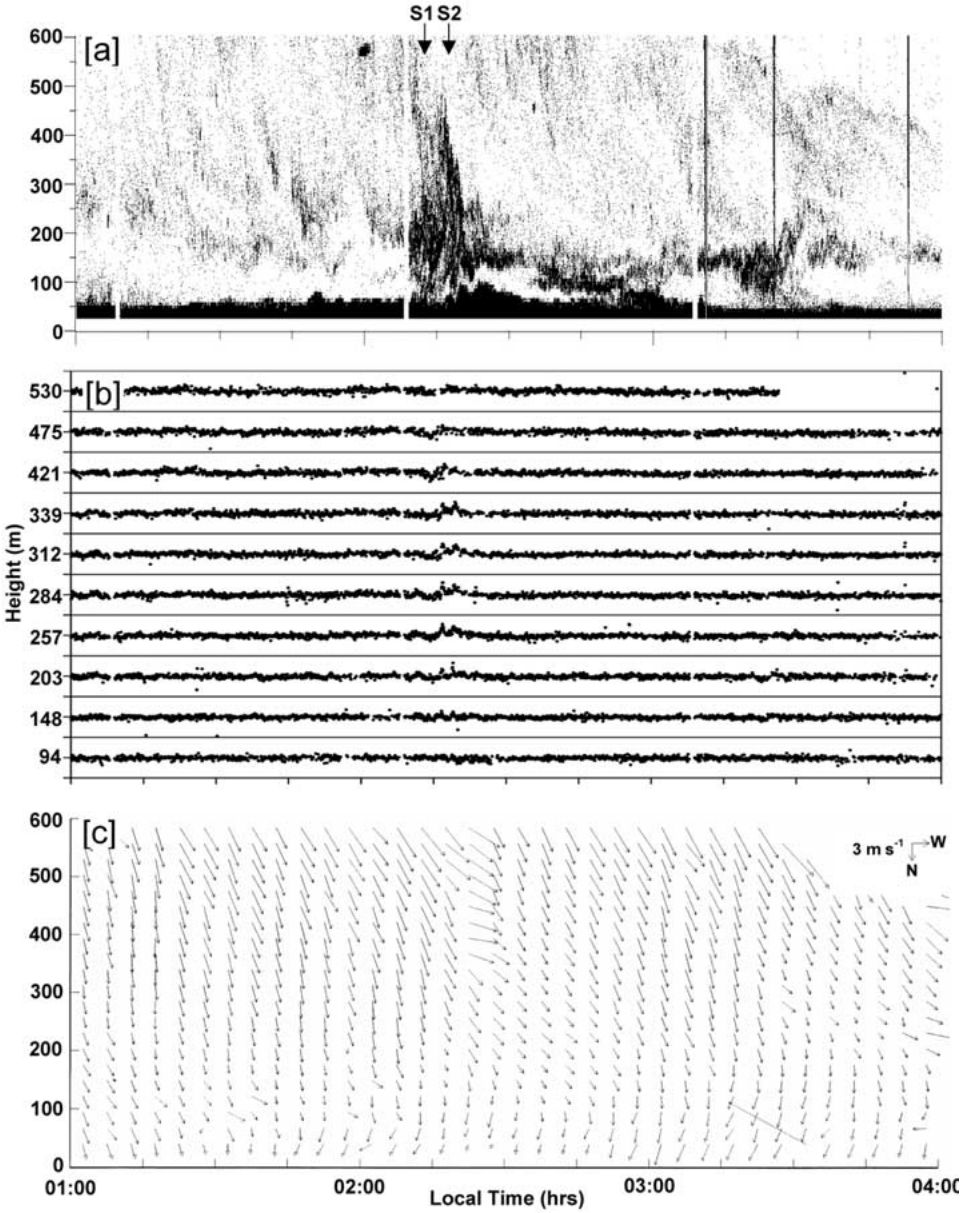

Figure 5. Same as Figure 3 but from 0100 to 0400 on April 16, 1996 at location P.

The horizontal wind field (Figure 5c) showed subtle change in the wind direction below 200 m around 0200 from predominantly north-west to north or north-north-east. The winds at higher levels were almost unchanged during the three-hour period, except for a brief period just before 0230.

3.1.4. *Wave Direction*

Several features of the sodar facsimile records and the horizontal wind field patterns seem to suggest that the same phenomenon was observed at the three locations, albeit with some variability in structure. The sudden appearance of the elevated layer at a few hundred metres height and its subsequent descent before the occurrence of the wave-associated disturbance were similar at each location. The horizontal winds were typically from north-west or north before the event. The wind shift to north or north-east after the event was also consistent at the three locations. The vertical velocity showed a greater variation at location U than at the other two locations.

The near simultaneous appearance of the wave-associated disturbance at locations U and M points out that it was propagating from north-west. The observation of a single solitary wave at location M suggests that the horizontal extension of the disturbance was limited. As mentioned earlier, the appearance of the wave at location P is devoid of wave shape on the facsimile record. Examination of the facsimile record at location U (Figure 3a) shows that the thickness of the no-echo region from S1 to the middle of S5 was nearly constant. The increase in the thickness of the no-echo region at the end of S5 can be taken as an indication that the recirculating air was being ejected from the rear of S5. The loss of recirculating air and the frictional losses at the surface affect both the amplitude and speed of propagation of solitary waves (Doviak et al., 1991). The urban canopy is highly inhomogeneous in both the horizontal and the vertical scales and the appearance of solitary waves without recirculating cells at location P can be attributed to these factors.

Identification of the possible source mechanism for the generation of the observed waves is difficult in the present study as the measurements are limited to three locations with no other supporting meso-meteorological data. The cold outflow from an earlier thunderstorm in the evening (Figure 2) established the stable layer in the UBL. Another cold outflow from a late-evening thunderstorm could be a source for the observed waves. The location of the experimental area is in the lower Tiber valley with mountains reaching above 1000 m height (Figure 1) so a drainage current from the surrounding mountains could also trigger such waves when the UBL is stable.

3.2. CASE 2: APRIL 18–19, 1996

The surface weather charts at 1300 on April 18 showed that an occluded front was present over Sicily and some parts of Sardinia and Meteosat images at 1700 (April 18) showed some isolated clouds over the west coast of the mainland.

There was sea-breeze activity over the experimental area during the day. The sea breeze first appeared at location P, as it is closer to the sea. The facsimile record (not presented here) shows a slant echo region extending up to 600 m height at the late morning. This is a typical depiction of sea-breeze fronts on sodar facsimile records (Kumar et al., 1986). The slow decrease of the slant echo region to heights below 400 m within few minutes might be due to Kelvin–Helmholtz billows that are known to exist on sea-breeze fronts (Simpson, 1994). The corresponding horizontal wind field shows that the winds were variable between north and east before the onset of the sea breeze. The sharp shift to south-west at the late morning indicates advection of marine air at the site. The change in the wind direction to south-west, as observed at the other two locations, indicated the onset of the sea breeze. It is known that the density current associated with a sea breeze has limited vertical extent and an elevated inversion is often established at the interface of the inflowing cool marine air and the free atmosphere above. The sodar records at the three locations for the remaining part of the day, showed that the inversion was variable between 400 and 500 m till about 1900. It can thus be assumed that the UBL was moderately stable up to few hundred metres due to the sea breeze.

3.2.1. *Location U*

The sodar facsimile record for the three-hour period from 2100 (April 18) to 0000 (April 19) is presented in Figure 6a. An elevated layer was observed between 100 and 150 m for about an hour from 2100. The interesting part of the record began at 2215 when a wave disturbance (marked as S1 and S2) of about 400 m amplitude arrived. The facsimile record shows no-echo regions within the waves indicating the existence of recirculation cells. The facsimile record showed multiple layers up to 300 m after the wave disturbance.

The time series of the vertical velocity for ten representative heights for the same period is presented in Figure 6b. The data were sparse at higher altitudes before the event. There were three waves between 2210 and 2230 with the middle wave having a vertical velocity variation from about $+3$ m s^{-1} to -2 m s^{-1}. The horizontal wind field presented in Figure 6c shows that the winds were south-east before the event and turned north-east after the event. The wind field showed a vortex-like pattern during the wave event. The existence of closed circulation cell in the form of a propagating vortex is considered as one of the characteristics of large amplitude solitary waves (Christie et al., 1978; Aigner et al., 1999).

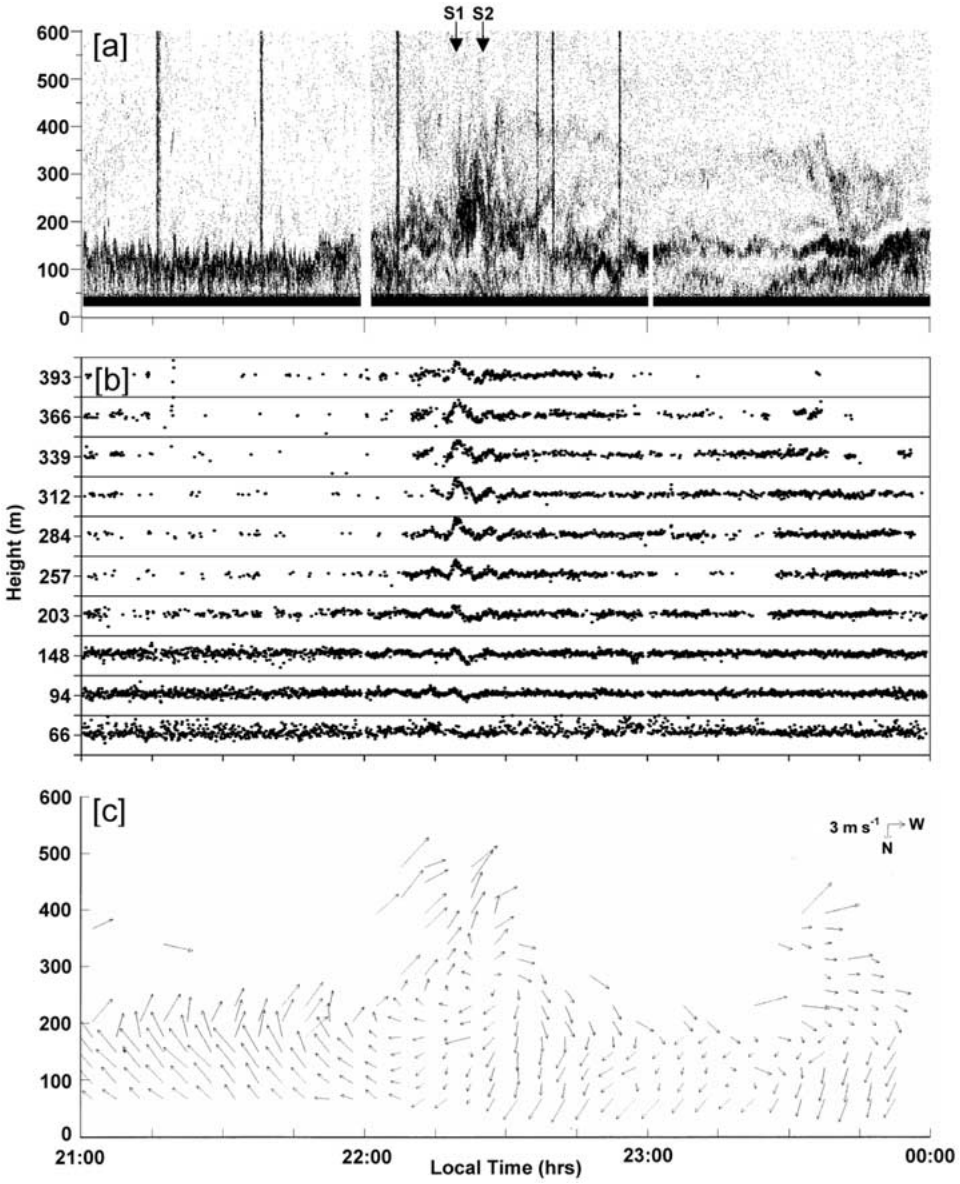

Figure 6. Same as Figure 3 but from 2100 (April 18, 1996) to 0000 (April 19, 1996) at location U.

3.2.2. *Location P*

The sodar facsimile record from 2300 (April 18) to 0200 (April 19) presented in Figure 7a shows an elevated layer at 500 m height at the beginning. The layer descended to 300 m in about 30 min. On its descent, the layer split into two with the top layer moving upwards while the lower layer hovered at around 250 m height. Another layer with some undulations appeared at 150 m height at 0000. A surface-

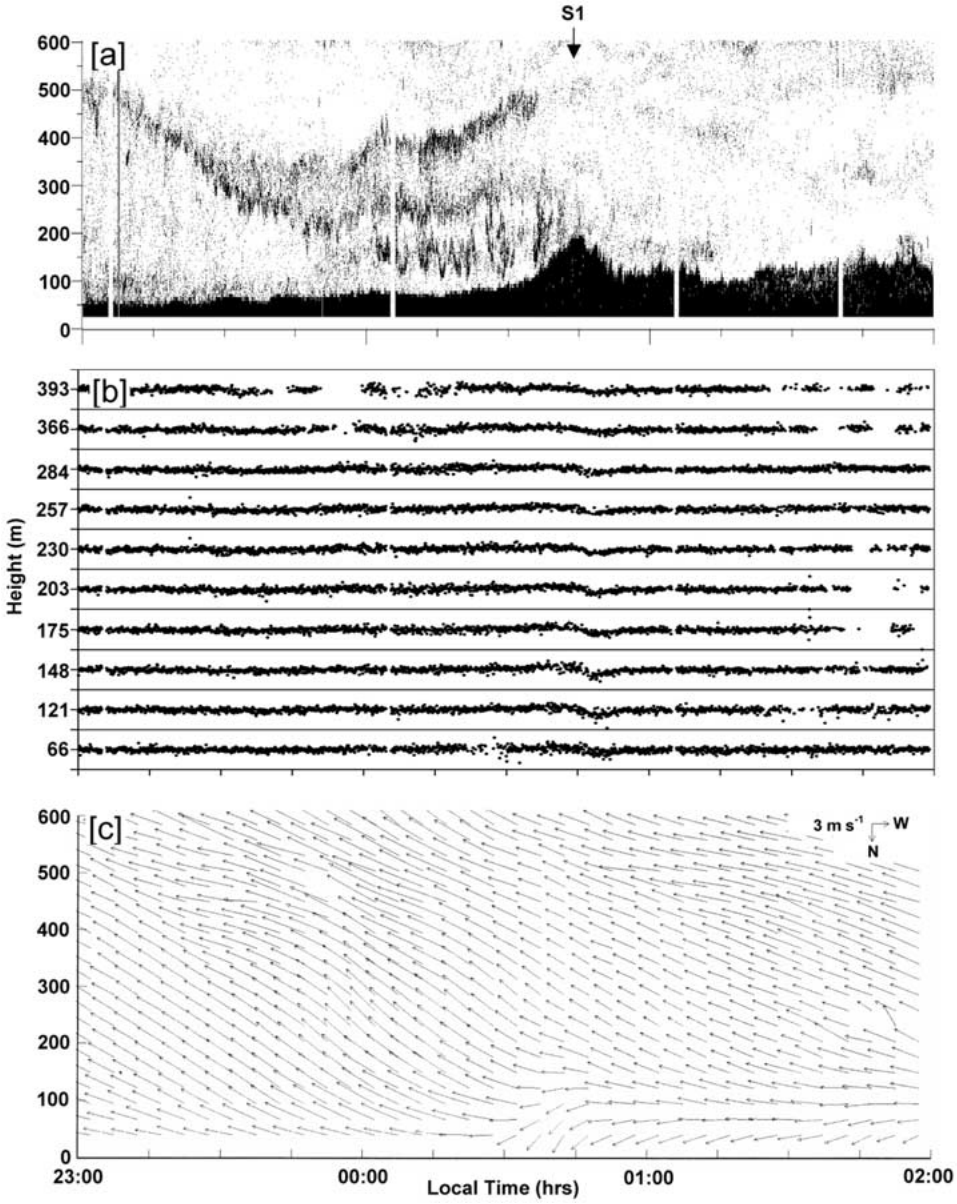

Figure 7. Same as Figure 3 but from 2300 (April 18, 1996) to 0200 (April 19, 1996) at location P.

based layer with an average depth of 50 m was present till 0030. It began to rise and reached a height of 200 m within about 5 min and descended in another 5 min. The surface-based layer then settled at an average height of 100 m during the rest of the observations.

The time series of vertical velocity for ten representative heights is shown in Figure 7b. The variation of the vertical velocity during the event between 0040 and 0050 appeared to be different compared to observations presented in previous sections. The vertical velocity was first seen decreasing to a peak negative value before reaching its pre-event value. This is typical of solitary waves of depression (Christie et al., 1978; Rottman and Einaudi, 1993). While no fully convincing explanation is possible with the limited data available in the present experiment, it may be pointed out that transformation of depression solitons to elevation solitons was observed in ocean internal solitons (Liu et al., 1998). The transformation is believed to be due to horizontal inhomogeneities in the thermocline. The bottom topography of the ocean plays a central role in either shoaling or deepening of the thermocline (Zheng et al., 2001). It is known that different land-use patterns in urban areas trigger the development of internal boundary layers in the UBL (Ching, 1985; Oke, 1987). The observed transformation of the wave in the present case may be attributed to the variation of the stable-layer thickness in the UBL.

The horizontal wind field presented in Figure 7c shows that the winds were mostly from south-east before the event. The winds below 200 m during the event turned north-east for a brief period of 20 min and later shifted to east. The winds above 200 m remained south-east during the entire period.

3.2.3. *Location M*

In the sodar facsimile record for the period 2300 (April 18) to 0200 (April 19) a surface-based layer, whose depth increased from 100 to 200 m, was observed for about 45 min from the beginning of the record (not presented here). The time series plot of vertical velocity shows two possible periods of wave activity: one from 0025 to 0030 and the other from 0140 to 0145. Both periods seem to be in consonance with the earlier observed behaviour of the vertical velocity during the solitary wave events. The horizontal wind field shows that the wind was from south-east or east all through the record except during the period from 0020 to 0050. Based on the vertical and horizontal wind fields, it is believed that the solitary wave observed at locations U and P appeared at this location at 0025.

3.2.4. *Wave Direction*

The time series of vertical velocity and horizontal wind field patterns aided in the detection of wave-associated disturbances at the three locations. The vertical wind variation was largest at location U. The horizontal wind was from either east or south-east at each location before the arrival of the waves and it typically turned to north-east at all locations during the wave disturbance. The change of the wind direction to north-east or east was consistent at the three locations after the wave disturbance. All these factors suggest that the observed wave-associated disturbance was the same at the three locations. Moreover, the simultaneous appearance of the disturbance at location M and P suggests that the disturbance was propagating from a north-east direction.

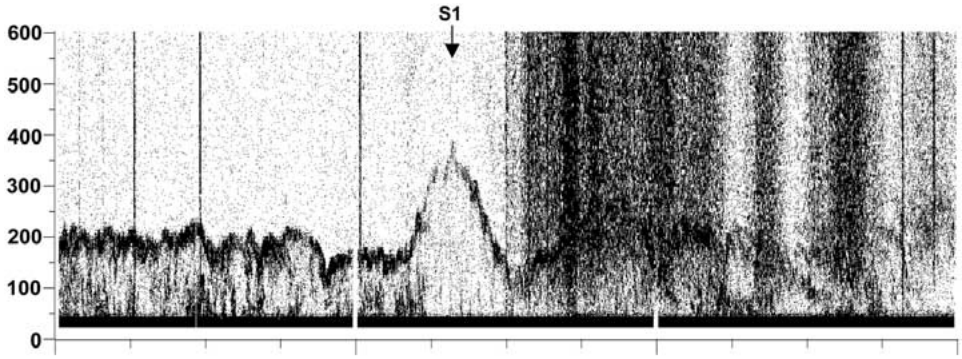

Figure 8. Same as Figure 3 but from 1300 to 1600 (November 23, 1996) at location U.

The source of these waves, also in this case, is not clear as there were no reports of thunderstorms in Rome or its surroundings. However, the surface relative humidity record showed a 20% decrease between 2100 and 2330 indicating that there was dry air advection over the experimental area. A cold outflow from a late evening thunderstorm or a drainage current originating from the surrounding mountains are possible sources.

3.3. Case 3: November 23, 1996

The surface weather charts showed a large and complex low pressure system moving eastwards from the Mediterranean sea. There were wide spread rain cells in many parts of central and southern Italy. The surface relative humidity changed very little from its previous night maximum. The peak daytime surface temperature was 11 °C.

The sodar facsimile record of the location U for the period from 1300 to 1600 (November 23) is shown in Figure 8. An elevated layer between 150 and 200 m with small undulations was seen till 1410. Some weak thermal plume activity was also observed below the elevated layer. The elevated layer rose quickly to a peak height of about 375 m and fell back between 1410 and 1430. The weak thermal plume activity that occurred till 1410 was almost absent during this event. The blackness of the record after the event marked the arrival of rain at the site.

The variation of vertical velocity during the wave event (not shown here) is similar to the other events discussed earlier. The amazing symmetry of the wave coupled with the absence of echoes within the wave indicates the presence of a recirculating cell. The horizontal wind field (not shown here) shows few measurements, but those available indicate that the winds were variable.

The sodar data at the other two locations did not show any wave-associated disturbance for this event and rain onset was almost simultaneous at all the three locations.

3.4. RECIRCULATING CELLS

The no-echo regions on the sodar facsimile records are a clear indication of the existence of recirculating cells with the wave, but the vertical cross section of the wind vector plot in the plane of wave propagation is traditionally used for this purpose (Doviak and Ge, 1984; Fulton et al., 1990). The 1-min averaged sodar wind profile measurements of one-hour duration for cases 1 and 2 at location U are selected for this analysis. The horizontal wind at each measurement height was divided into components parallel and perpendicular to the wave direction. The vertical and parallel components of the wind were combined as described by Cheung and Little (1990) and are plotted in Figure 9. It may be recalled here that the recirculating air is acoustically smooth and seldom produces echoes. As expected, the vector plots in Figure 9b could only delineate the flow around the cells, which were identified on corresponding facsimile records presented in Figures 3a and 7a. The circulation pattern in Figure 9b between 2215 and 2230 h up to 500 m shows two cells. The circulation patterns in Figure 9a are less clear but the variability of the wind vector from 0015 to about 0045 is still sufficient to locate the recirculating cells.

3.5. VERTICAL VELOCITY VARIATION

The vertical velocity is one of the principal parameters used to identify wave phenomena in the ABL and it is often believed that each class of waves leaves its characteristic imprint on the vertical velocity field (Rottman and Einaudi, 1993). In all the cases so far discussed, and more specifically in the cases where the wave was believed to transport recirculating air, the vertical velocities were observed to initially rise to a maximum positive velocity followed by a smooth decrease to a peak negative velocity at every measurement height. It may be interesting to see the vertical variation of the vertical velocity during the wave events. Christie and Muirhead (1983) theoretically calculated the vertical wind field for a fairly large amplitude solitary wave, with a closed circulation cell, propagating in a strongly stable surface-based inversion of 400 m depth. The vertical velocity is found to increase monotonically from the ground to the top of the internal closed circulation. For an isothermal waveguide of 2 km depth with constant shear, Rottman and Einaudi (1993) computed the vertical velocity field for a wave of 200 m amplitude propagating at the fairly high speed of 27 m s^{-1}. The largest vertical velocities are found at the top of the waveguide. It may be mentioned here that few observational studies seem to report the vertical structure of vertical velocities during wave events. Cheung and Little's (1990) observations of solitary waves in a shallow nocturnal boundary layer showed that the vertical velocity increased with height from the surface to the top of the closed circulation. An attempt is made here to verify whether our observed solitary waves in the UBL also show this behaviour. Six wave periods were identified from the sodar facsimile records from the three events at location U when the internal circulation was clearly visible. The peak

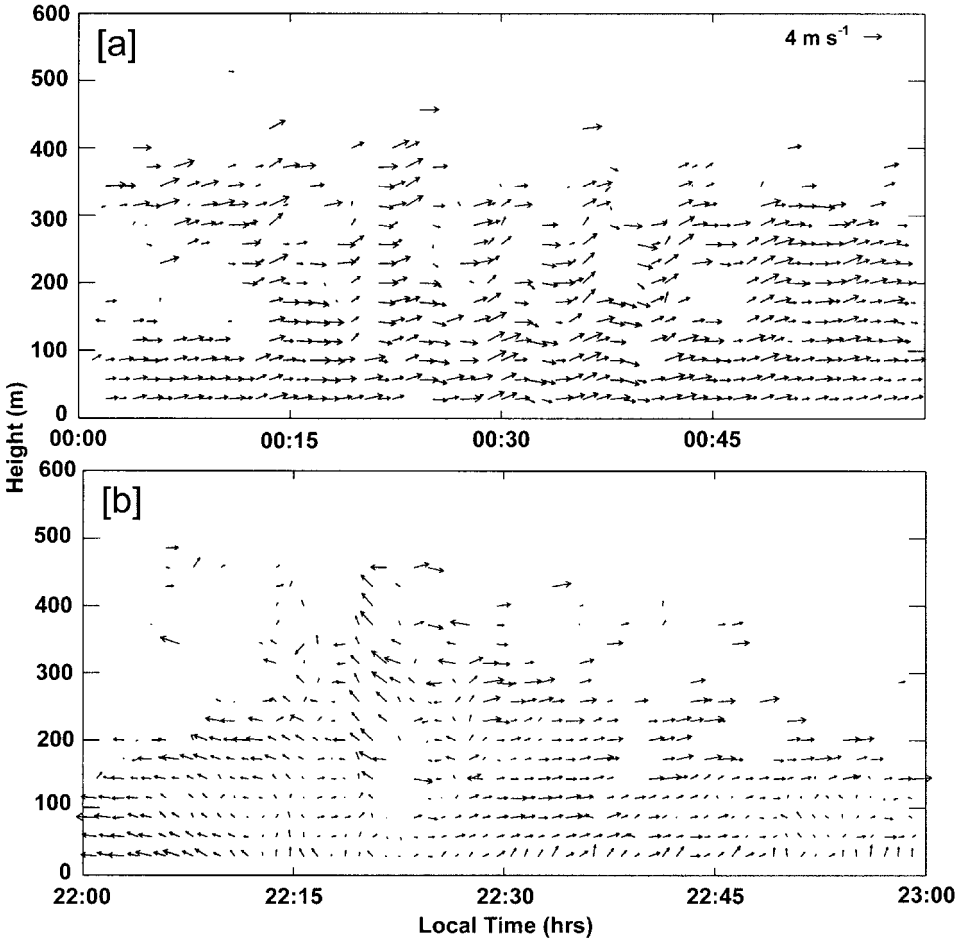

Figure 9. Wind flow pattern in the plane of wave propagation on (a) April 16, 1996 from 0000 to 0100, and (b) April 18, 1996 from 2200 to 2300 at location U.

positive velocities at each height of measurement during the six selected wave periods were identified and plotted against height in Figure 10. The height was normalised with the height of the internal circulation measured directly from the sodar facsimile records (the height of the no-echo region within the wave). Despite some spread in the data, a clear increase of vertical velocity with height is visible up to the normalised height of 0.8. The peak positive vertical velocities lie in the region between 0.7 and 1.2 normalised height. The velocities were mostly around 2 m s^{-1} between those heights. Considering the inhomogeneities that exist in UBLs in both horizontal and vertical scales, besides the necessarily simplified theoretical calculations, the agreement between the observed and the predicted trends by the theory of solitary waves is satisfactory.

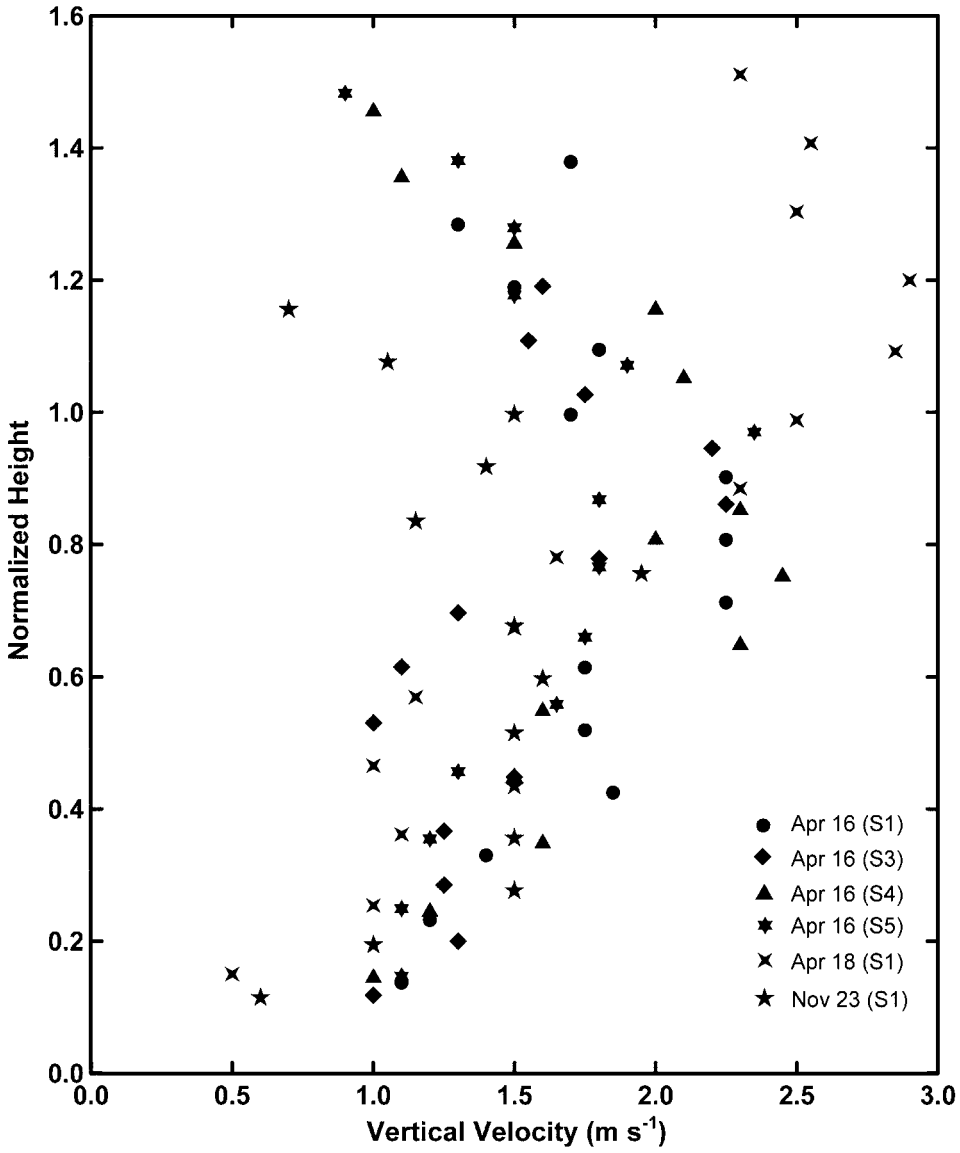

Figure 10. Vertical velocity variation with height for the selected six waves.

3.6. AMPLITUDE-WAVELENGTH RELATIONSHIP

The weakly nonlinear theory of waves, often referred to as BDO (Benjamin–Davis–Ono) theory, deals with solitary waves propagating in a waveguide whose depth is relatively larger than the wave amplitudes (Ono, 1975; Rottman and Einaudi, 1993; Rottman and Grimshaw, 2001). The inverse relation between amplitude and wavelength for weakly nonlinear waves begins to breakdown once the waves

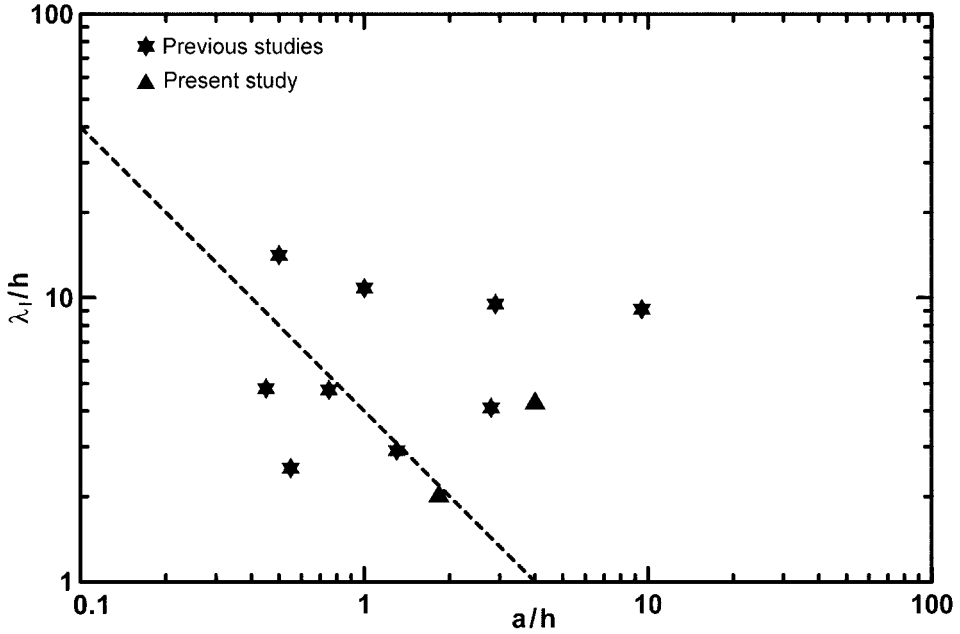

Figure 11. Wavelength versus amplitude for the present two cases of April 16 and 18, 1996. The other data are taken from the previous studies mentioned in Section 3.6.

start to carry recirculation cells (Tung et al., 1982). The amplitude-wavelength scaling proposed by Koop and Butler (1981) provides the domain of validity for different solitary wave theories. As the solitary waves observed in the present experiment were believed to transport recirculation cells and thus qualify for fully nonlinear treatment, it may be interesting to validate the present observations in this domain. As discussed earlier, the solitary waves detected by the sodar at location U showed recirculation cells on all three occasions. The data for cases 1 and 2 only were used for the amplitude-wavelength scaling computations, as case 3 was not observed at other locations.

It is conventional to define the wavelength of solitary waves as half of the distance between half-amplitude points, which are defined as points where wave amplitude attains half of its maximum value. The time elapsed between these half-amplitude points was measured from the sodar facsimile records (zoomed) and converted into distance by multiplying with the trace velocity of the wave (Cheung and Little, 1990). The trace velocity was measured by taking the time of arrival of the wave at the three locations. The wavelengths were calculated using the relation, $\lambda = v\tau/2$, where v is the trace velocity and τ is the time interval between half-amplitude points on the facsimile record. The observed wavelengths for the two cases were then converted to integral scale wavelengths, $\lambda_I = \pi\lambda/2$ (Koop and Butler, 1981). The integral scale wavelength and the amplitude normalised to the depth of the stratified layer, h, and are plotted in Figure 11. The straight line repres-

ents the weakly nonlinear case according to BDO theory in which the wavelength decreases with the amplitude. It must be recalled that the BDO theory begins to break down at $a/h > 0.5$ when the air within the wave begins to recirculate (Tung et al., 1982). The wave begins to transport air from its initiating disturbance at $a/h > 1$. Also plotted in Figure 11 are data from previous studies of atmospheric solitary waves by Goncharov and Matveyev (1982), Doviak et al. (1991), Cheung and Little (1990), Rottman and Einaudi (1993), and Rees and Rottman (1994) for comparison. Although the data points are limited to two cases, the agreement between theoretical prediction and present observations appears good. The data also seem to be in close agreement with previous studies. The data show that in the waves studied, the wavelength is larger or at least comparable to the values assumed in the weakly nonlinear theory of solitary waves.

4. Conclusions

The simultaneous operation of three Doppler sodar systems in the Rome region enabled the detection of solitary waves in the UBL. Of the three events reported here, two were observed at all three locations. The waveguide necessary for the propagation of solitary waves in these two cases was believed to be established by a cold outflow from a previous thunderstorm for case 1 and by the sea-breeze circulation for case 2. The source mechanisms for the generation of the three events could not be established directly, but thunderstorm cold outflows or drainage flows from nearby mountain slopes are possible active sources.

The sodar facsimile records were primarily used to identify the events. Some of the observed solitary waves showed no-echo regions indicating the existence of recirculation cells within the waves. The vertical velocity variation during the wave events was typically similar to that of elevation solitons. However, in one case, it appeared as an elevation soliton at two locations and as a depression soliton at the other location. The present data are limited and do not permit a convincing explanation for this behaviour, but such transformations are known to occur in ocean internal solitons. The development of internal boundary layers due to different land-use patterns in the urban area can generate horizontal inhomogeneities in the thermocline, which, in turn, can transform solitons. Several other features of the observations share the characteristics of solitary waves. The vertical velocity is found to increase almost monotonically up to the height of the recirculation cells. The relation between the amplitude and the wavelength of the two events indicates that the observed waves are close to a strongly nonlinear regime. The loss of recirculation cells and the retardation due to friction by the urban canopy are two possible reasons for the steep decrease in amplitudes as they propagated over the observational network.

It may not be possible to draw any major conclusions from this study as the data set is limited to three events and the variability of the observed waves is too

large, but the significance lies perhaps in the rarity of their occurrence. Although the generating mechanisms of solitary waves appear simple and might exist quite frequently, observations of solitary waves in the atmosphere are still sparse. The fact that only three events were observed in more than one year of continuous measurements might indicate that solitary waves are not as ubiquitous as often believed, and might require a combination of environmental settings for their generation and propagation. As the waves are expected to change their form while propagating in the UBL, it is sometimes difficult to recognize the wave structure on the sodar facsimile records. A dense network of Doppler sodars would be advisable for future measurements.

Acknowledgements

The authors are grateful to Dr. G. Mastrantonio (IFA/CNR) for help in sodar data analysis. One of the authors (MPR) received financial assistance from the 'ICTP Programme for Training and Research in Italian Laboratories', Trieste, Italy.

References

Aigner, A., Broutman, D., and Grimshaw, R.: 1999, 'Numerical Simulation of Internal Solitary Waves with Vortex Cores', *Fluid Dyn. Res.* **25**, 315–333.

Casadio, S., di Sarra, A., Fiocco, G., Fuà, D., Lena, F., and Rao, M. P.: 1996, 'Convective Characteristics of the Nocturnal Urban Boundary Layer as Observed with Doppler Sodar and Raman Lidar', *Boundary-Layer Meteorol.* **79**, 375–391.

Cheung, T. K. and Little, C. G.: 1990, 'Meteorological Tower, Microbarograph Array, and Sodar Observations of Solitary-Like Waves in the Nocturnal Boundary Layer', *J. Atmos. Sci.* **47**, 2516–2536.

Cheung, T. K., Little, C. G., and Ramm, H. E.: 1990, 'Thin Acoustic Scattering Layers Observed in the Low Marine Boundary Layer', *J. Atmos. Sci.* **47**, 2537–2545.

Ching, J. K. S.: 1985, 'Urban-Scale Variations of Turbulence Parameters and Fluxes', *Boundary-Layer Meteorol.* **33**, 335–361.

Christie, D. R.: 1992, 'The Morning Glory of the Gulf of Carpentaria: A Paradigm for Non-Linear Waves in the Lower Atmosphere', *Aust. Meteorol. Mag.* **41**, 21–60.

Christie, D. R. and Muirhead, K. J.: 1983, 'Solitary Waves: A Low-Level Wind Shear Hazard to Aviation', *Int. J. Aviat. Safety* **1**, 169–190.

Christie, D. R., Muirhead, K. J., and Clarke, R. H.: 1981, 'Solitary Waves in the Lower Atmosphere', *Nature* **293**, 46–49.

Christie, D. R., Muirhead, K. J., and Hales, A. L.: 1978, 'On Solitary Waves in the Atmosphere', *J. Atmos. Sci.* **35**, 805–825.

Clarke, J. C.: 1998, 'An Atmospheric Undular Bore along the Texas Coast', *Mon. Wea. Rev.* **126**, 1098–1100.

Clifford, S. F., Kaimal, J. C., Lataitis, R. J., and Strauch, R. G.: 1994, 'Ground-Based Remote Profiling in Atmospheric Studies: An Overview', *Proc. IEEE* **82**, 312–355.

Doviak, R. J. and Ge, R. S.: 1984, 'An Atmospheric Solitary Gust Observed with a Doppler Radar, a Tall Tower and a Surface Network', *J. Atmos. Sci.* **41**, 2559–2573.

Doviak, R. J., Chen, S. S., and Christie, D. R.: 1991, 'A Thunderstorm-Generated Solitary Wave Observation Compared with Theory for Nonlinear Waves in a Sheared Atmosphere', *J. Atmos. Sci.* **48**, 87–111.

Fulton, R., Zrnic, D. S., and Doviak, R. J.: 1990, 'Initiation of a Solitary Wave Family in the Demise of a Nocturnal Thunderstorm Density Current', *J. Atmos. Sci.* **47**, 319–337.

Goncharov, V. P. and Matveyev, A. K.: 1982, 'Observations of Nonlinear Waves on an Atmospheric Inversion', *Izv. Atmos. Ocean. Phys.* **18**, 61–64.

Hall, F. F., Neff, W. D., and Frazier, T. V.: 1976, 'Wind Shear Observations in Thunderstorm Density Currents', *Nature* **264**, 408–411.

Koop, C. G. and Butler, G.: 1981, 'An Investigation of Internal Solitary Waves in a Two-Fluid System', *J. Fluid Mech.* **112**, 225–251.

Kumar, A. R., Rao, M. P., and Murthy, J. S. R.: 1986, 'The Effect of Sea Breeze on Atmospheric Stability as Observed with Acoustic Sounder', *Boundary-Layer Meteorol.* **35**, 303–311.

Liu, A. K., Chang, Y. S., Hsu, M. K., and Liang, N. K.: 1998, 'Evolution of Nonlinear Internal Waves in the East and South China Seas', *J. Geophys. Res.* **103**, 7995–8008.

Mastrantonio, G. and Argentini, S.: 1997, 'A Modular PC-Based Multiband Sodar System', in S. P. Singal (ed.), *Acoustic Remote Sensing Applications*, Narosa Publishing House, New Delhi, pp. 105–116.

Mastrantonio, G. and Fiocco, G.: 1982, 'Accuracy of Wind Velocity Determinations with Doppler Sodar', *J. Appl. Meteorol.* **21**, 820–830.

Menhofer, A., Smith, R. K., Reeder, M. J., and Christie, D. R.: 1997, 'Morning-Glory Disturbances and the Environment in which They Propagate', *J. Atmos. Sci*. **54**, 1712–1725.

Oke, T. R.: 1987, *Boundary Layer Climates*, Routledge, London, 435 pp.

Ono, H.: 1975, 'Algebraic Solitary Waves in Stratified Fluids', *J. Phys. Soc. Japan* **39**, 1082–1091.

Rees, J. M. and Rottman, J. W.: 1994, 'Analysis of Solitary Disturbances over an Antarctic Ice Shelf', *Boundary-Layer Meteorol.* **69**, 285–310.

Rottman, J. W. and Einaudi, F.: 1993, 'Solitary Waves in the Atmosphere', *J. Atmos. Sci.* **50**, 2116–2136.

Rottman, J. W. and Grimshaw, R.: 2001, *Atmospheric Internal Solitary Waves*, Monograph, Department of Mathematical Sciences, Loughborough University, Leicestershire, U.K, 28 pp.

Simpson, J. E.: 1994, *Sea Breeze and Local Winds*, Cambridge University Press, Cambridge, 234 pp.

Szantai, A., Desalmand, F., Desbois, M., Picon, L., Randriamiarisoa, H., and Senoussi, E.: 2000, 'Meteosat-5 Observations of Low-Level Wave Clouds along the West Coast of India during INDOEX', in *The 2000 EUMETSAT Meteorological Satellite Data Users' Conference*, 25 May–2 June, 2000, Bologna, Italy.

Tung, K. K., Chan, T. F., and Kubota, T.: 1982, 'Large Amplitude Internal Waves of Permanent Form', *Stud. Appl. Math.* **66**, 1–44.

Zheng, Q., Klemas, V., Yan, X.H., and Pan, J.: 2001, 'Nonlinear Evolution of Ocean Internal Solitons Propagating along an Inhomogeneous Thermocline', *J. Geophys. Res.* **106**, 14083–14094.

Zheng, Q., Yan, X. H., Liu, W. T., Klemas, V., Greger, D., and Wang, Z.: 1998, 'Solitary Wave Packet in the Atmosphere Observed from Space', *Geophys. Res. Lett.* **25**, 3559–3562.